Prediction of pathological nodal involvement by CT-based Radiomic features of the primary tumor in patients with clinically node-negative peripheral lung adenocarcinomas

Ying Liu
Department of Radiology, Tianjin Medical University Cancer Institute and Hospital, National Clinical Research Center for Cancer, Key Laboratory of Cancer Prevention and Therapy, Tianjin's Clinical Research Center for Cancer, Tianjin
Department of Cancer Imaging and Metabolism, H. Lee Moffitt Cancer Center and Research Institute, 12902 Magnolia Drive, Tampa, FL, USA

Jongphil Kim
Department of Biostatistics and Bioinformatics, H. Lee Moffitt Cancer Center and Research Institute, 12902 Magnolia Drive, Tampa, FL, USA

Yoganand Balagurunathan
Department of Cancer Imaging and Metabolism, H. Lee Moffitt Cancer Center and Research Institute, 12902 Magnolia Drive, Tampa, FL, USA

Samuel Hawkins
Department of Computer Sciences and Engineering, University of South Florida, Tampa, FL, USA

Olya Stringfield
Department of Cancer Imaging and Metabolism, H. Lee Moffitt Cancer Center and Research Institute, 12902 Magnolia Drive, Tampa, FL, USA

Matthew B. Schabath
Department of Cancer Epidemiology, H. Lee Moffitt Cancer Center and Research Institute, 12902 Magnolia Drive, Tampa, FL, USA

Qian Li
Department of Radiology, Tianjin Medical University Cancer Institute and Hospital, National Clinical Research Center for Cancer, Key Laboratory of Cancer Prevention and Therapy, Tianjin's Clinical Research Center for Cancer, Tianjin
Department of Cancer Imaging and Metabolism, H. Lee Moffitt Cancer Center and Research Institute, 12902 Magnolia Drive, Tampa, FL, USA

Fangyuan Qu and Shichang Liu
Department of Radiology, Tianjin Medical University Cancer Institute and Hospital, National Clinical Research Center for Cancer, Key Laboratory of Cancer Prevention and Therapy, Tianjin's Clinical Research Center for Cancer, Tianjin

Alberto L. Garcia
Department of Cancer Imaging and Metabolism, H. Lee Moffitt Cancer Center and Research Institute, 12902 Magnolia Drive, Tampa, FL, USA

Zhaoxiang Ye
Department of Radiology, Tianjin Medical University Cancer Institute and Hospital, National Clinical Research Center for Cancer, Key Laboratory of Cancer Prevention and Therapy, Tianjin's Clinical Research Center for Cancer, Tianjin

Robert J. Gillies[a)]
Department of Cancer Imaging and Metabolism, H. Lee Moffitt Cancer Center and Research Institute, 12902 Magnolia Drive, Tampa, FL, USA
Department of Radiology, H. Lee Moffitt Cancer Center and Research Institute, 12902 Magnolia Drive, Tampa, FL, USA

(Received 5 January 2018; revised 7 March 2018; accepted for publication 23 March 2018; published 29 April 2018)

Purpose: The purpose of this study was to investigate the potential of computed tomography (CT) based radiomic features of primary tumors to predict pathological nodal involvement in clinically node-negative (N0) peripheral lung adenocarcinomas.
Methods: A total of 187 patients with clinical N0 peripheral lung adenocarcinomas who underwent preoperative CT scan and subsequently received systematic lymph node dissection were retrospectively reviewed. 219 quantitative 3D radiomic features of primary lung tumor were extracted; meanwhile, nine radiological semantic features were evaluated. Univariate and multivariate logistic regression analysis were used to explore the role of these features in predicting pathological nodal involvement. The areas under the ROC curves (AUCs) were compared between multivariate logistic regression models.
Results: A total of 153 patients had pathological N0 status and 34 had pathological lymph node metastasis. On univariate analysis, fissure attachment and 17 radiomic features were significantly associated with pathological nodal involvement. Multivariate analysis revealed that semantic features

of pleural retraction (P = 0.048) and fissure attachment (P = 0.023) were significant predictors of pathological nodal involvement (AUC = 0.659); and the radiomic feature F185 (Histogram SD Layer 1) (P = 0.0001) was an independent prognostic factor of pathological nodal involvement (AUC = 0.73). A logistic regression model produced from combining radiomic feature and semantic feature showed the highest AUC of 0.758 (95% CI: 0.685–0.831), and the AUC value computed by fivefold cross-validation method was 0.737 (95% CI: 0.73–0.744).

Conclusions: Features derived on primary lung tumor described by semantic and radiomic could provide information of pathological nodal involvement in clinical N0 peripheral lung adenocarcinomas. [https://doi.org/10.1002/mp.12901]

Key words: adenocarcinoma, lung cancer, lymph node, metastasis, tomography, X ray computed

Abbreviations

NSCLC non-small cell lung cancer
CT computed tomography
PET positron emission tomography
18F-FDG PET/CT
18F-fluorodeoxyglucose positron emission tomography/computed tomography
SUV standard uptake value
EBUS-TBNA
endobronchial ultrasound transbronchial nodal aspiration cytology
GGO ground glass opacity
FDR false discovery rate
OR odds ratios
CI confidence intervals
PCA principle component analysis
ROC receiver operating characteristic
AUC area under the curve

1. INTRODUCTION

Despite recent improvements in diagnostic and therapeutic strategies, lung cancer remains the leading cause of cancer-related death throughout the world. Non-small cell lung cancer (NSCLC) patients account for about 80%–85% of all lung cancer patients, for whom treatment is mainly determined according to TNM staging system.[1] The status of mediastinal or hilar lymph node is the most significant factor to determine TNM stage, and accurate identification of positive lymph node is critical for selection of optimal therapy and determination of patient prognosis.[2] It has been shown[3] that 5-year survival rate of patients without lymph node metastasis (N0) is about 56%, compared with only 38% for patients with pulmonary lymph node metastasis (N1). Complete lymph node excision with microscopic evaluation is thought to be the most accurate method for determining lymph node metastasis. However, the extent of lymph node removal and the efficacy benefit of lymph node dissection are controversial;[4–7] the more lymph nodes are dissected, the better local control due to removal of micro-metastases and decreased risk of residual lesions, but it also causes greater trauma for the patients, such as prolonged air leaks and excessive chest tube drainage. Therefore, a method to predict the presence of undetected lymph node metastasis would be helpful to eliminate pseudo negative cases, and systematic lymph node dissection should be considered in these patients even with a small tumor.

Several noninvasive procedures including computed tomography (CT) and positron emission tomography (PET) are used for diagnosing nodal involvement in lung cancer. Conventional CT interpretation relies on primarily size criteria to characterize lymph nodes. A short-axis diameter bigger than 10 mm was considered as the standard threshold for abnormal nodes.[8–10] However, lymph node size alone is not a reliable parameter for the evaluation of metastatic involvement in patients with NSCLC; metastases have been found in up to 20% of small nodes in patients with clinical stage cT1N0 and cT2N0.[11] This results in low accuracy of CT in the diagnosis of lymph node malignancy.[12–14] A prospective study has confirmed that 18F-fluorodeoxyglucose positron emission tomography/computed tomography (18F-FDG PET/CT) had a higher diagnostic accuracy in lymph node characterization than anatomical imaging.[15] According to a histologically verified meta-analysis of PET/CT for the nodal staging of NSCLC,[16] the pooled sensitivity was 0.62 (95% CI: 0.54–0.70), widely ranging from 0.13 to 0.98, and the specificity ranged between 0.72 and 0.98 with an overall estimated specificity of 0.92 (0.88–0.95) for node-based data; which means specificity is satisfactory, while sensitivity remains disappointing.

Several studies[9,17–21] have been undertaken to investigate the relationship between standard uptake value (SUV) of primary lung cancer lesions and node involvement, and the results showed that SUV_{max} of the primary tumor might be an independent predictor of regional lymph node metastasis in patients with NSCLC. CT is widely used as the standard of care procedure used routinely for assessing NSCLC, and the vast majority of lung cancer patients undergo only chest CT as their diagnostic procedure. The predictive image markers generated in CT would improve clinical diagnosis; they are less expensive and consume less time. Radiomics has the capacity to extract additional features from medical images, providing improvements of image analysis.[22] Thus, we conducted this study to evaluate if CT-based radiomic features of the primary tumor could provide useful information in predicting lymph node metastases in clinical N0 peripheral lung adenocarcinomas.

2. MATERIALS AND METHODS

2.A. Patient selection

Our local institutional review board waived the requirement for individual patient consent for the use of data for this retrospective study. We retrospectively reviewed the medical records of patients with NSCLC treated with surgery between December 2012 and March 2014. 221 patients were identified according to the following inclusion criteria: (a) patients with primary lung adenocarcinoma underwent lobectomy or pneumonectomy with systematic lymph node dissection of both hilar and mediastinal lymph nodes; (b) acquisition of preoperative thin-section CT scan and the location of the lung tumor was peripheral (tumor involving subsegmental bronchus or smaller airway); (c) clinical N stage was N0. Clinical N0 stage was defined preoperatively by three radiologists according to thin-section chest CT images in a mediastinal window setting (width, 350 HU; level, 40 HU) if the hilar and mediastinal lymph nodes were no larger than 10 mm in short-axis diameter. Majority class was used as the final decision in case of disagreement. We excluded all patients receiving preoperative induction therapy (n = 9), those underwent any type of preoperative invasive mediastinal staging such as endobronchial ultrasound transbronchial nodal aspiration cytology (EBUS-TBNA) or mediastinoscopy (n = 11), those with multiple primary lesions (n = 4), and those the duration between CT examination and subsequence surgery exceeded 1 month (n = 7). Additional patients (n = 3) were excluded for uncertainty in tumor extent during segmentation. Finally, the remaining 187 patients constituted the study population.

The following parameters were collected for all the patients: gender, age, smoking status, primary tumor histologic subtype and pathologic stage. For the smoking status, patients were categorized as never smokers or smokers which included former or current smokers. All resected tumor specimens were examined and classified based on the 2011 IASLC/ATS/ERS classification system.[23] The dissected lymph nodes were stained by hematoxylin and eosin and then histologically examined. These pathological examinations were all performed by experienced pulmonary pathologists at the same hospital. TNM classification and tumor staging were performed according to the 8th edition of the staging system published by the Union for International Cancer Control and the American Joint Committee on Cancer.[24]

2.B. CT protocol and tumor segmentation

CT studies were obtained on multi-detector CT systems (Siemens Somatom 64, Siemens Medical Solutions; GE Light speed 16 or GE Discovery 750 HD, GE Medical Systems) with a breath-held acquisition of the entire thorax, 120 kVp, 150–200 mA or with automatic tube current modulation, pitch 0.969:1. The reconstruction thickness and interval was 1.5 mm for the 64-detector scanner, and 1.25 mm for the 16-detector scanner and Discovery CT750 HD scanner.

Tumors were volumetrically segmented by two radiologists with different experience in thoracic oncological imaging using Definiens Developer XD© (Munich, Germany) (Figure S1). Tumor segmentation results were confirmed by each other. The workflow for this semi-automatic approach which contained the following four steps named pre-processing, semi-automated correction of the pulmonary boundary, click and grow, and manual refinement and generation of lesion statistics, was described in detail in our previous studies[25–28] and 219 features were extracted (Table S1).

2.C. CT image evaluation/semantic features

Three consultant radiologists (one radiologist with 6 yr of experience in CT imaging of thoracic malignancies and the other two radiologists with 3 yr of experience) who were blinded to the clinical information and pathologic results reviewed the CT images to score semantic features for all patients independently. In case of disagreement, consensus was achieved by group discussion. CT images were analyzed in lung window setting (width, 1500 HU; level, −600 HU). CT findings for each lesion included: (a) attenuation, (b) spiculation, (c) pleural retraction, (d) concavity, (e) air bronchogram, (f) bubble-like lucency, (g) fissure attachment, (h) pleural attachment, and (i) lobe location (Figure S2).

According to the findings on thin-section CT, tumor attenuation was allocated to one of three groups: pure ground glass opacity (GGO), mixed GGO, and pure solid tumors. GGO was defined as an area of a slight homogeneous increase in density that did not obscure the underlying vascular markings.[29] A mixed GGO tumor was defined as one with both GGO and solid components, and a pure solid tumor was defined as having only solid components without any ground glass appearance. Spiculation was recorded as no, fine, or coarse. Fine spiculation was defined as very fine linear strands extending radially 1–2 mm beyond a lesion, and coarse spiculation was defined by the presence of 2 mm or thicker strands extending from the nodule margin into the lung parenchyma without reaching the pleural surface.[30] Concavity, also known as notch, was defined as V-shaped indentation of the border deeper than 3 mm,[31] and it was reported as no, slight, or deep. For all the other five CT features, including air bronchogram, bubble-like lucency, pleural retraction, pleural attachment, and fissure attachment, presence or absence was used to describe the tumor. Air bronchogram was defined as the tube like or branched air structure within the tumor. Bubble-like lucency was defined as the presence of air in the tumor at the time of diagnosis, prior to biopsy or treatment. Pleural retraction was defined as a linear structure originating from the tumor and extending to the pleural surface, with the pleura retracted toward the tumor. Pleural/fissure attachment was defined as the tumor margin obscured by the pleura or fissure.

2.D. Statistical analysis

All statistical analyses were performed using SAS software (version 9.4, Cary, NC, USA). Continuous variables were reported as medians and ranges, while categorical variables were reported as counts and percentages. Pearson's correlation analysis was performed to identify redundant features, thus 122 radiomic features (absolute value of Pearson correlation coefficients >0.95) were eliminated. Then we apply the same procedure to eliminate the redundant features among those 97 remaining features. Finally, 86 radiomic features were selected as potential predictors of nodal involvement (Table S2). False discovery rate (FDR)[32] was used to account for multiple testing, we set a q-value of 0.1 to screen out radiomic features in order to control false discovery, remaining features were used for building multivariable model. We used a relaxed significance limits in the univariate analysis (P <0.1, FDR q-value <0.1) both for radiomic and semantic features that were incorporated in building multivariable model. Features with P-value or q-value of <0.1 were incorporated into building multivariable model. Backward elimination method was used to select the final predictive model; at each step, feature with P >0.1 was eliminated. Odds ratios (OR) as estimates of relative risk along with 95% confidence intervals (CI) were obtained for each risk factor. Furthermore, principle component analysis (PCA) was performed based on top five radiomic features. Receiver operating characteristic (ROC) curves for each model were constructed and the area under the curve (AUC) and 95% CI was calculated. Goodness of fit for logistic regression models was estimated by Hosmer-Lemeshow test to examine the calibration of the model.[33] Comparisons between two AUCs were made by the nonparametric approach of the DeLong method.[34] Fivefold cross-validation with 100 replications was performed to evaluate the performance of the final model. A two-sided P <0.05 was regarded as statistically significant. Decision curve analysis was conducted to evaluate prediction models in terms of their clinical usefulness.

3. RESULTS

Characteristics of study population are summarized in Table S3. The cohort comprised 77 men and 110 women, with a median age of 59 yr. Acinar predominant adenocarcinoma accounted for most of the tumors (n = 79, 42.2%), followed by lepidic predominant (n = 50, 26.7%), solid predominant (n = 28, 15.0%), and the other histological subtypes of adenocarcinoma (n = 30, 16.0%). Regarding tumor stage, most were stage I (n = 145, 77.5%). Lobectomy was performed in 183 patients, and pneumonectomy in 4 patients. Among all of the clinical N0 peripheral lung adenocarcinoma patients, 153 (81.8%) had pathological N0 status and 34 (18.2%) had pathological nodal involvement. The patients were divided into two groups based on the results of pathological nodal involvement: pathologic lymph node (LN) positive vs pathologic LN negative. Pathologic stage was significant different between these two groups (P < 0.0001), as early stage was more common in pathologic LN negative group (98.0%) than pathologic LN positive group (26.5%). No other clinicopathological characteristics were statistically significant different between these two groups (Table I).

Table II summarized differences in pathologic LN negative and positive groups using semantic features. No significant differences were seen between semantic features and pathologic nodal involvement except for fissure attachment (P = 0.025). There were significantly more patients (47.1%) with fissure attachment in LN positive group compared to LN negative group (26.8%). Multivariable analysis demonstrated that pleural retraction (P = 0.048, OR = 0.44, 95% CI: 0.20–0.99) and fissure attachment (P = 0.023, OR = 2.45, 95% CI: 1.13–5.31) were significant parameters for predicting nodal involvement. The AUC of this model was 0.659, and the model was well fitted (P = 0.60 by Hosmer and Lemeshow test). Then pure GGO and mix GGO were grouped together (Pure and mix GGO vs Pure solid), and there was significant different in the univariable model (P = 0.034) but not in multivariable model (P = 0.103) and was eliminated from the final model.

The association between radiomic features and pathologic nodal involvement was investigated. In the univariate analysis, 17 radiomic features were found to be significantly correlated with nodal malignancy (Table III, Table S4, and Figure S3). However, in multivariable analysis, F185 (Histogram SD Layer 1) was the only independent predictor of pathologic nodal involvement (P = 0.0001, OR = 0.35, 95% CI: 0.21–0.59) with an AUC of 0.726. The Hosmer and Lemeshow test showed no significant difference between

TABLE I. Clinical Characteristics of patients by their nodal involvement.

Clinicopathological features	Pathologic LN negative (n = 153)	Pathologic LN positive (n = 34)	P-value
Gender			
Male	66 (43.1%)	11 (32.4%)	0.34
Female	87 (56.9%)	23 (67.6%)	
Age			
Median (range)	59 (37-80)	60.5 (30-76)	0.36
Smoking history			
Smokers	63 (41.2%)	14 (41.2%)	1
Non-smokers	90 (58.8%)	20 (58.8%)	
Histological subtype[a]			
Lepidic predominant adenocarcinomas	47 (30.7%)	6 (17.6%)	0.15
Others	106 (69.3%)	28 (82.4%)	
Pathological stage			
Early stage (I or II)	150 (98%)	9 (26.5%)	<0.0001
Advanced stage (III or IV)	3 (2%)	25 (73.5%)	

[a]Histologic subtype was categorized as lepidic predominant adenocarcinomas (adenocarcinoma *in situ*, minimally invasive adenocarcinoma, and lepidic predominant invasive adenocarcinoma) and other subtypes of dominant histologic findings (acinar, papillary, micropapillary, and solid predominant as well as variants of invasive adenocarcinoma).

TABLE II. Comparison of semantic features across LN negative and positive groups.

Parameter	Pathologic LN negative (n = 153)	Pathologic LN positive (n = 34)	*P*-value
Attenuation			
Pure GGO	8 (5.2%)	0 (0%)	0.10
Mixed GGO	49 (32%)	6 (17.6%)	
Pure solid	96 (62.7%)	28 (82.4%)	
Spiculation			
No spiculation	35 (22.9%)	9 (26.5%)	0.83
Fine spiculation	57 (37.3%)	11 (32.4%)	
Coarse spiculation	61 (39.9%)	14 (41.2%)	
Pleural retraction			
Absence	79 (51.6%)	24 (70.6%)	0.056
Presence	74 (48.4%)	10 (29.4%)	
Concavity			
No concavity	7 (4.6%)	2 (5.9%)	0.54
Slight concavity	94 (61.4%)	24 (70.6%)	
Deep concavity	52 (34%)	8 (23.5%)	
Air bronchogram			
Absence	66 (43.1%)	13 (38.2%)	0.70
Presence	87 (56.9%)	21 (61.8%)	
Bubble-like lucency			
Absence	58 (37.9%)	16 (47.1%)	0.34
Presence	95 (62.1%)	18 (52.9%)	
Fissure attachment			
Absence	112 (73.2%)	18 (52.9%)	0.025
Presence	41 (26.8%)	16 (47.1%)	
Pleural attachment			
Absence	119 (77.8%)	26 (76.5%)	0.82
Presence	26 (17%)	8 (23.5%)	
Lobe location			
Right upper	51 (33.3%)	10 (29.4%)	0.99
Right middle	14 (9.2%)	4 (11.8%)	
Right lower	27 (17.6%)	6 (17.6%)	
Left upper	40 (26.1%)	9 (26.5%)	
Left lower	21 (13.7%)	5 (14.7%)	

observed and expected pathologic nodal involvement with malignancy (P = 0.25).

The association between two semantic features (pleural retraction and fissure attachment) and top five radiomic features is investigated, and fissure attachment is highly associated with all top five features (Table S5).

Then another prognostic model was built by combining semantic and radiomic features (Table S6). Absence of pleural retraction and lower feature value of F185 were correlated with high odds of nodal involvement of malignancy. The highest AUC of 0.758 was achieved by combination of semantic and radiomic features (Fig. 1), and the AUC value computed by fivefold cross-validation with 100 replications was 0.737 (95% CI: 0.73–0.744). This model was also well fitted (P = 0.35 by Hosmer and Lemeshow test). There was significant improvement of AUC compared to the model generated with only semantic features (P = 0.016); however, the difference did not reach statistical significance compared to the model produced from radiomic feature alone (P = 0.14) (Table IV). The decision curve analysis for these three models is presented in Fig. 2. The decision curve showed that if the threshold probability of predicting nodal involvement is between 20% and 30%, using the model that combined

TABLE III. Univariate analysis of the relationship between radiomic features and pathologic nodal involvement.

		Odds Ratio				
			95% CI			
Feature	*P*-value	Point	Lower	Upper	AUC	*q*-value
F185 (Histogram-SD- Layer 1)	0.0001	0.35	0.21	0.59	0.73	0.005
F187 (Histogram-Entropy- Layer 1)	0.0001	0.44	0.29	0.67	0.73	0.005
F5 (StdDev [HU])	0.0003	0.37	0.22	0.64	0.70	0.010
F4 (Mean [HU])	0.003	7.61	1.97	29.31	0.70	0.069
F18 (9 g-3D-Max-Dist-COG-to-Border)	0.005	1.70	1.18	2.45	0.64	0.079
F188	0.008	1.55	1.12	2.15	0.71	0.12
F48	0.011	1.59	1.11	2.28	0.67	0.14
F15	0.013	1.57	1.10	2.24	0.63	0.13
F199	0.014	0.43	0.22	0.84	0.69	0.13
F16	0.021	1.50	1.06	2.12	0.62	0.18
F14	0.026	1.44	1.05	1.99	0.63	0.19
F191	0.026	0.52	0.29	0.93	0.66	0.19
F1	0.031	1.48	1.04	2.12	0.62	0.19
F30	0.032	0.62	0.40	0.96	0.62	0.19
F139	0.034	0.61	0.38	0.96	0.60	0.19
F135	0.038	0.60	0.37	0.97	0.59	0.20
F37	0.043	1.44	1.01	2.04	0.62	0.22

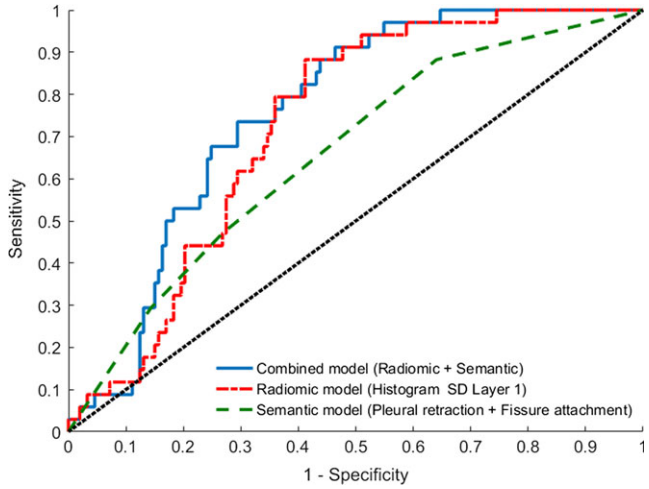

FIG. 1. Receiver operating characteristic (ROC) curves from multivariate analysis of sementic model (Pleural retraction + Fissure attachment), radiomic model (F185 (Histogram SD Layer 1) alone), and combined model (F185 (Histogram SD Layer 1) alone + Pleural retraction). [Color figure can be viewed at wileyonlinelibrary.com]

TABLE IV. Comparison of predictive performance between different prognostic models.

Feature	AUC			
		95% CI		
	Point	Lower	Upper	*P*-value[a]
F185 (Histogram SD Layer 1) + Pleural retraction	0.758	0.685	0.831	
F185 (Histogram SD Layer 1)	0.726	0.650	0.802	0.14
Pleural retraction + Fissure attachment	0.659	0.567	0.751	0.016

[a]*P*-value was computed by the comparison with F185 + Pleural retraction using the DeLong method.

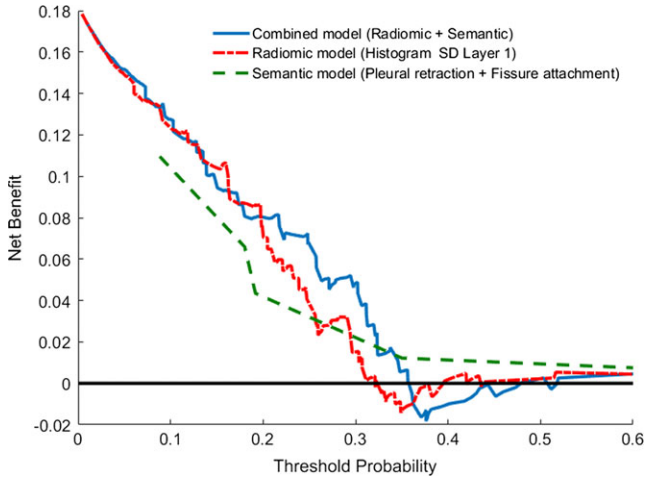

FIG. 2. Decision curve for pathological nodal involvement prediction in clinical N0 peripheral lung adenocarcinomas: Comparison of three models. The *y*-axis measures the net benefit. The blue line represents the model with semantic and radiomic features. The red dashed line represents the model with radiomic features. The green dashed line represents the model with semantic features. The black line represents the assumption that no patients have nodal involvement. [Color figure can be viewed at wileyonlinelibrary.com]

semantic and radiomic features to predict nodal involvement adds more benefit than either the semantic model or the radiomic model.

According to PCA analysis, PC1 and PC2 explained 69.2% and 18.8% of variation, respectively.

$$\begin{aligned} PC1 = {} & 0.522187 \times F185 + 0.502444 \times F187 \\ & + 0.454285 \times F5 - 0.451671 \times F4 \\ & - 0.253947 \times F18. \end{aligned}$$

$$\begin{aligned} PC2 = {} & 0.041721 \times F185 - 0.109188 \times F187 \\ & + 0.410455 \times F5 - 0.160764 \times F4 \\ & + 0.889955 \times F18. \end{aligned}$$

When PC1 and PC2 were incorporated into the model, PC2 was not significant ($P = 0.81$), and PC1 was considered as the predictor of nodal involvement ($P < 0.0001$, OR = 0.53, 95% CI: 0.40–0.72) with an AUC of 0.735 (95% CI: 0.659–0.81). Model was well fitted by Hosmer and Lemeshow test ($P = 0.17$). The multivariate prognostic model was built by combining semantic features with radiomic features (semantics and PC1). Unfortunately, semantic features of fissure attachment ($P = 0.87$) and pleural retraction ($P = 0.102$) were eliminated from the model. No statistical difference in AUC was seen between PC1 alone and the model produced from combination of semantics with radiomics (F185 + Pleural retraction) ($P = 0.35$).

4. DISCUSSION

Lymph node metastasis is an important prognostic factor in patients with NSCLC. Although thoracic thin-section CT is widely used in preoperative evaluation of nodal status, it is still challenging to distinguish metastatic lymph nodes from benign lymph nodes in clinical practice, especially for those lymph nodes with a short-axis diameter of less than 10 mm, which are always classified as negative for metastasis before surgery. Even for PET/CT, which was considered to be superior to that of CT alone for the preoperative staging of NSCLC, potential lymph node involvement may not be detected, and it was reported that 51 (19.2%) of 265 patients with clinical N0 NSCLC had pathological lymph node involvement in a recent study.[9] In our study, all patients were considered as cN0 stage and no lymphadenopathy could be found on CT images. Of note, enlargement is not necessarily a salient feature of malignant, and with our data, 34 of them had pathologic lymph node metastasis, leading to 18.2% false-negative rates, indicating that prediction of metastasis lymph node based on size criteria alone is not accurate.

Quantitative radiomics research has been focused on characterizing primary tumors, studying its reproducibility and relating to clinical, pathological outcome.[35–37] In these findings, size, shape descriptors along with texture described by HU histogram characteristics (standard deviation, entropy, kurtosis), Runlength, Cooccurrence, some wavelets, Laws features were shown to be prognostics and predictive.[22,25,38–41] In a prior study,[42] tumor size on computed tomography ($P = 0.006$) and tumor consistency (solid tumor vs GGO tumor) ($P < 0.001$) were independent predictors for lymph node metastasis. Given that GGO might be the only component of some tumor, our study took a slightly different approach, defining tumor attenuation as pure GGO, mixed GGO, and pure solid instead of solid tumor or GGO tumor (a tumor with at least 50% GGO component). We found out that there was a trend toward higher rate of pure solid tumor in the pathologic LN positive group compared to negative group, although this was not statistically significant ($P = 0.10$); meanwhile, none of the tumors of pure GGO had lymph node metastasis. We then grouped pure GGO and mix GGO together, and found that it was significant in the univariable model ($P = 0.034$); however, not significant in multivariable model ($P = 0.103$).

Univariate analysis revealed that longest tumor diameter (F1) was significant predictor ($P = 0.031$). Some of these findings were consistent with the majority of published literature.[42–45] However, tumor size was not associated with nodal involvement with malignancy on multivariate analysis in our

study. It is notable that textural (HU histogram) and shape characeteristics are better descriptors of nodal malignancy. Prior studies concur with our findings, that texture characteristics are related to recurrence and possible nodal status in NSCLC[46,47] and in other cancers.[48] In this study, more semantic features of primary lung tumor were evaluated, and we found that tumor with fissure attachment were more likely to have metastatic LNs, and one more feature "pleural retraction" was significant at multivariate analysis. Usually, the presence of pleural retraction is considered as a strong factor for poor prognosis;[49] thus, we hypothesized that tumor with pleural retraction might have higher incidence of developing lymph node metastasis. Somewhat unexpectedly, absence of pleural retraction is an indicator of pathological nodal involvement with malignancy. Although the exact reason for this is not entirely clear, it may be due to that some cases with pleural retraction may not accompanied by pleural invasion, which is supported by the findings that pleural retraction was found in 83 of the 105 cases, but pleural invasion was found in only 25 pathological samples; in such cases, the pleura may have been retracted proximal to the tumor but not yet invaded, or peripheral atelectasis due to airway obstruction by the tumor may have been observed.[50] It could also be related to the fact that we limited the patients to those clinical N0 peripheral lung adenocarcinomas, which was rather different from previous studies.

Radiomics provides large amounts of advanced quantitative imaging features which are extracted and analyzed from medical images. Whole-lesion analysis was used in these studies, which provides a more comprehensive picture of lesion heterogeneity. Seven radiomic features that fall in three broad groups (morphological features, histogram features, and high order texture features) of primary lung tumor had significant association with pathological nodal involvement; and Pixel Intensity Histogram feature (F185) was an independent predictor in multivariate analysis. This model showed better performance (AUC = 0.726) than model generated with semantic features (AUC = 0.659). It seems that radiomic analysis of the primary tumor could lead to a better performance than routine measure done by radiologists which mainly focusing on size criteria in predicting nodal involvement. As the goal of this study is to build predictive model for nodal involvement, the association between two semantic features (fissure attachment and pleural retraction) and top five radiomic features is investigated by simple logistic regression. The fissure attachment is highly associated with all top five features, and this explains the reason why it was eliminated in the final multivariable model.

We further utilized the radiomic features and semantic features jointly to predict pathological nodal involvement. The multivariate model with semantic feature "pleural retraction" and radiomic feature "Histogram SD" demonstrated the highest AUC (AUC = 0.758), which outperformed the model with semantic features alone (P = 0.016). Meanwhile, we applied decision curve analysis which requires only the dataset on which the models are tested to evaluate and compare three different prediction models. Since Radiomics analysis allows high-throughput extraction of quantitative features from biomedical images which can reflects underlying pathophysiology, we hypothesized that Radiomic features of the primary tumor could reflect the biologic malignant potential of lung cancer; therefore, assessment of the noninvasive radiomic features of the primary tumor could serve as a more informative analysis method and the prediction model which incorporates both semantic and radiomic features may provide a new way for preoperative evaluating the risk of lymph node metastasis in patients with clinical N0 peripheral lung adenocarcinomas.

Our study has several limitations. First, this study was retrospective in design with a limited number of patients in a single Institute. Second, in order to have a more accurate assessment of lymph node metastasis, only patients received lobectomy or pneumonectomy with systematic lymph node dissection were included in this study, so there may have been selection bias. Third, this study examined patients with peripheral lung adenocarcinomas, since central bronchogenic tumors often cause post-obstructive pneumonia and induce atelectasis, which is difficult to be differentiated from tumor as both of them appear as solid dense shadows on CT images. Fourthly, there is relatively small number of patients with malignant lymph node in our group, and this situation was dictated by the demographic characteristics of our cohort; that is, only patients with clinical N0 peripheral lung adenocarcinomas. Finally, not all of the patients in the cohort received FDG-PET/CT scan preoperatively, we did not compare the results to the current standard of PET CT. Further validation with larger series is needed to confirm our preliminary results.

5. CONCLUSIONS

Our preliminary study revealed association between primary tumor CT features and pathological nodal involvement in clinical N0 peripheral lung adenocarcinomas. Combined evaluation of semantic and radiomic features could improves prediction of the risk of a node's involvement with malignancy, and this modality could be easily added to clinical use due to its non-invasive nature.

ACKNOWLEDGMENTS

This work was supported by the National Cancer Institute (grants U01 CA143062), and National Natural Scientific Foundation of China (No. 81501443). This work has been supported in part by the Biostatistics Core Facility at the Moffitt Cancer Center & Research Institute; a National Cancer Institute designated Comprehensive Cancer Center (5P30CA076292-17).

CONFLICTS OF INTEREST

RJG is a consultant and shareholder in HealthMyne, Inc. and oncology-specific PACS system. No other authors of this

manuscript have relationships with any companies, whose products or services may be related to the subject matter of the article.

[a]Author to whom correspondence should be addressed. Electronic mail: robert.gillies@moffitt.org; Telephone: 813-745-8355.

REFERENCES

1. Ettinger DS, Akerley W, Bepler G, et al. Non–small cell lung cancer. *J Natl Compr Canc Netw*. 2010;8:740–801.
2. Doddoli C, Aragon A, Barlesi F, et al. Does the extent of lymph node dissection influence outcome in patients with stage I non-small-cell lung cancer? *Eur J Cardiothorac Surg*. 2005;27:680–685.
3. Rusch VW, Crowley J, Giroux DJ, et al. The IASLC Lung Cancer Staging Project: proposals for the revision of the N descriptors in the forthcoming seventh edition of the TNM classification for lung cancer. *J Thorac Oncol*. 2007;2:603–612.
4. Allen MS, Darling GE, Pechet TT, et al. Morbidity and mortality of major pulmonary resections in patients with early-stage lung cancer: initial results of the randomized, prospective ACOSOG Z0030 trial. *Ann Thorac Surg*. 2006;81:1013–1020.
5. Wu Yl, Huang ZF, Wang SY, Yang XN, Ou W. A randomized trial of systematic nodal dissection in resectable non-small cell lung cancer. *Lung Cancer*. 2002;36:1–6.
6. Darling GE, Allen MS, Decker PA, et al. Randomized trial of mediastinal lymph node sampling versus complete lymphadenectomy during pulmonary resection in the patient with N0 or N1 (less than hilar) non–small cell carcinoma: results of the American College of Surgery Oncology Group Z0030 Trial. *J Thorac Cardiovasc Surg*. 2011;141:662–670.
7. Zhong W, Yang X, Bai J, Yang J, Manegold C, Wu Y. Complete mediastinal lymphadenectomy: the core component of the multidisciplinary therapy in resectable non-small cell lung cancer. *Eur J Cardiothorac Surg*. 2008;34:187–195.
8. Kirchner J, Broll M, Muller P, et al. CT differentiation of enlarged mediastinal lymph node due to anthracosis from metastatic lymphadenopathy: a comparative study proven by endobronchial US-guided transbronchial needle aspiration. *Diagn Interv Radiol*. 2015;21:128–133.
9. Miyasaka Y, Suzuki K, Takamochi K, Matsunaga T, Oh S. The maximum standardized uptake value of fluorodeoxyglucose positron emission tomography of the primary tumour is a good predictor of pathological nodal involvement in clinical N0 non-small-cell lung cancer. *Eur J Cardiothorac Surg*. 2013;44:83–87.
10. Schaarschmidt BM, Buchbender C, Nensa F, et al. Correlation of the Apparent Diffusion Coefficient (ADC) with the Standardized Uptake Value (SUV) in Lymph Node Metastases of Non-Small Cell Lung Cancer (NSCLC) Patients Using Hybrid 18F-FDG PET/MRI. *PLoS ONE*. 2015;10:e0116277.
11. Toloza EM, Harpole L, Detterbeck F, McCrory DC. Invasive staging of non-small cell lung cancer: a review of the current evidence. *CHEST J*. 2003;123(1_suppl):157S–166S.
12. Dales RE, Stark RM, Raman S. Computed tomography to stage lung cancer. *Am Rev Respir Dis*. 1990;141:1096–1101.
13. Beadsmoore C, Screaton N. Classification, staging and prognosis of lung cancer. *Eur J Radiol*. 2003;45:8–17.
14. Budiawan H, Cheon GJ, Im H-J, et al. Heterogeneity analysis of 18F-FDG uptake in differentiating between metastatic and inflammatory lymph nodes in adenocarcinoma of the lung: comparison with other parameters and its application in a clinical setting. *Nucl Med Mol Imaging*. 2013;47:232–241.
15. Perigaud C, Bridji B, Roussel JC, et al. Prospective preoperative mediastinal lymph node staging by integrated positron emission tomography–computerised tomography in patients with non-small-cell lung cancer. *Eur J Cardiothorac Surg*. 2009;36:731–736.
16. Pak K, Park S, Cheon GJ, et al. Update on nodal staging in non-small cell lung cancer with integrated positron emission tomography/computed tomography: a meta-analysis. *Ann Nucl Med*. 2015;29:409–419.
17. Li M, Wu N, Zheng R, et al. Primary tumor PET/CT [18F] FDG uptake is an independent predictive factor for regional lymph node metastasis in patients with non-small cell lung cancer. *Cancer Imaging*. 2012;12:566.
18. Nakamura H, Saji H, Marushima H, et al. Standardized uptake values in the primary lesions of non-small-cell lung cancer in FDG-PET/CT can predict regional lymph node metastases. *Ann Surg Oncol*. 2015;22:1388–1393.
19. Muto J, Hida Y, Kaga K, et al. Use of maximum standardized uptake value on fluorodeoxyglucose positron-emission tomography in predicting lymph node involvement in patients with primary non-small cell lung cancer. *Anticancer Res*. 2014;34:805–810.
20. Li X, Zhang H, Xing L, et al. Predictive value of primary fluorine-18 fluorodeoxyglucose standard uptake value for a better choice of systematic nodal dissection or sampling in clinical stage IA non–small-cell lung cancer. *Clin Lung Cancer*. 2013;14:568–573.
21. Xu Z-Q, Xie L-J, Fan W, Duan X-B, Cheng M-H. Risk factors for mediastinal lymph node metastasis in non-small-cell lung cancer by PET/CT. *Nucl Med Commun*. 2014;35:466–471.
22. Parmar C, Velazquez ER, Leijenaar R, et al. Robust radiomics feature quantification using semiautomatic volumetric segmentation. *PLoS ONE*. 2014;9:e102107.
23. Travis WD, Brambilla E, Noguchi M, et al. International association for the study of lung cancer/american thoracic society/european respiratory society: international multidisciplinary classification of lung adenocarcinoma: executive summary. *Proc Am Thorac Soc*. 2011;8:381–385.
24. Goldstraw P, Chansky K, Crowley J, et al. The IASLC lung cancer staging project: proposals for revision of the TNM stage groupings in the forthcoming (Eighth) edition of the TNM classification for lung cancer. *J Thorac Oncol*. 2016;11:39–51.
25. Balagurunathan Y, Kumar V, Gu Y, et al. Test–retest reproducibility analysis of lung CT image features. *J Digit Imaging*. 2014;27:805–823.
26. Gu Y, Kumar V, Hall LO, et al. Automated delineation of lung tumors from CT images using a single click ensemble segmentation approach. *Pattern Recogn*. 2013;46:692–702.
27. Velazquez ER, Aerts HJ, Gu Y, et al. A semiautomatic CT-based ensemble segmentation of lung tumors: Comparison with oncologists' delineations and with the surgical specimen. *Radiother Oncol*. 2012;105:167–173.
28. Liu Y, Kim J, Balagurunathan Y, et al. Radiomic features are associated with EGFR mutation status in lung adenocarcinomas. *Clin Lung Cancer*. 2016;17:441–448.e446.
29. Aoki T, Tomoda Y, Watanabe H, et al. Peripheral lung adenocarcinoma: correlation of thin-section CT findings with histologic prognostic factors and survival 1. *Radiology*. 2001;220:803–809.
30. Zwirewich C, Vedal S, Miller R, Müller N. Solitary pulmonary nodule: high-resolution CT and radiologic-pathologic correlation. *Radiology*. 1991;179:469–476.
31. Lee HJ, Goo JM, Lee CH, et al. Predictive CT findings of malignancy in ground-glass nodules on thin-section chest CT: the effects on radiologist performance. *Eur Radiol*. 2009;19:552–560.
32. Benjamini Y. Discovering the false discovery rate. *J Roy Stat Soc*. 2010;72:405–416.
33. Hosmer DW, Lemesbow S. Goodness of fit tests for the multiple logistic regression model. *Commun Stat Theory Methods*. 1980;9:1043–1069.
34. Delong ER, Delong DM, Clarkepearson DL. Comparing the areas under two or more correlated receiver operating characteristic curves: a nonparametric approach. *Biometrics*. 1988;44:837–845.
35. Aerts HJ, Velazquez ER, Leijenaar RT, et al. Decoding tumour phenotype by noninvasive imaging using a quantitative radiomics approach. *Nat Commun*. 2014;5:4006.
36. Balagurunathan Y, Gu Y, Wang H, et al. Reproducibility and prognosis of quantitative features extracted from CT images. *Transl Oncol*. 2014;7:72–87.
37. Ganeshan B, Goh V, Mandeville HC, Ng QS, Hoskin PJ, Miles KA. Non-small cell lung cancer: histopathologic correlates for texture parameters at CT. *Radiology*. 2013;266:326–336.
38. Grove O, Berglund AE, Schabath MB, et al. Quantitative computed tomographic descriptors associate tumor shape complexity and

intratumor heterogeneity with prognosis in lung adenocarcinoma. *PLoS ONE*. 2015;10:e0118261.
39. Hawkins S, Wang H, Liu Y, et al. Predicting malignant nodules from screening CTs. *J Thorac Oncol*. 2016;11:2120–2128.
40. Liu Y, Kim J, Balagurunathan Y, et al. Radiomic features are associated with EGFR mutation status in lung adenocarcinomas. *Clin Lung Cancer*. 2016;17:441–448.
41. Zhao B, Tan Y, Tsai W-Y, et al. Reproducibility of radiomics for deciphering tumor phenotype with imaging. *Sci Rep*. 2016;6:23428.
42. Wang L, Jiang W, Zhan C, et al. Lymph node metastasis in clinical stage IA peripheral lung cancer. *Lung Cancer*. 2015;90:41–46.
43. Tsutani Y, Miyata Y, Nakayama H, et al. Appropriate sublobar resection choice for ground glass opacity-dominant clinical stage IA lung adenocarcinoma: wedge resection or segmentectomy. *Chest*. 2014;145:66–71.
44. Cho S, Song IH, Yang HC, Kim K, Jheon S. Predictive factors for node metastasis in patients with clinical stage I non-small cell lung cancer. *Ann Thorac Surg*. 2013;96:239–245.
45. Takamochi K, Nagai K, Yoshida J, et al. Pathologic N0 status in pulmonary adenocarcinoma is predictable by combining serum carcinoembryonic antigen level and computed tomographic findings. *J Thorac Cardiovasc Surg*. 2001;122:325–330.
46. Coroller TP, Agrawal V, Narayan V, et al. Radiomic phenotype features predict pathological response in non-small cell lung cancer. *Radiother Oncol*. 2016;119:480–486.
47. Huynh E, Coroller TP, Narayan V, et al. Associations of radiomic data extracted from static and respiratory-gated CT scans with disease recurrence in lung cancer patients treated with SBRT. *PLoS ONE*. 2017;12:e0169172.
48. Zhou Y, He L, Huang Y, et al. CT-based radiomics signature: a potential biomarker for preoperative prediction of early recurrence in hepatocellular carcinoma. *Abdom Radiol (NY)*. 2017;42:1695–1704.
49. Yoshino I, Nakanishi R, Kodate M, et al. Pleural retraction and intratumoral air-bronchogram as prognostic factors for stage I pulmonary adenocarcinoma following complete resection. *Int Surg*. 2000;85:105–112.
50. Ikehara M, Saito H, Kondo T, et al. Comparison of thin-section CT and pathological findings in small solid-density type pulmonary adenocarcinoma: prognostic factors from CT findings. *Eur J Radiol*. 2010;81:189–194.

SUPPORTING INFORMATION

Additional Supporting Information may be found online in the supporting information tab for this article.

Table S1. 219 radiomic features extracted from Definiens, details of the features deferred to our prior publications.[1,2]
Table S2. Radiomic features included in final analysis.
Table S3. Characteristics of patients.
Table S4. Univariate analysis of the relationship between radiomic features and pathologic nodal involvement.
Table S5. Association between two semantic features and top five radiomic features.
Table S6. Multivariable logistic regression analysis of semantic features combined with radiomic features predicting nodal involvement.
Figure S1. Example of CT images showing segmentation results. The tumor boundary of each slice was shown in green outline.
Figure S2. Examples of CT images demonstrating typical semantic features: (a) pure GGO; (b) mixed GGO; (c) pure solid; (d) fine spiculation; (e) coarse spiculation; (f) pleural retraction; (g) slight concavity; (h) deep concavity; (i) air bronchogram; (j) bubble-like lucency; (k) fissure attachment; and (l) pleural attachment.
Figure S3. Boxplots comparing the top 5 radiomic features between pathologic LN negative and positive groups. (a) F4 (Mean [HU]); (b) F5 (StdDev [HU]); (c) F18 (9g-3D-Max-Dist-COG-to-Border); (d) F185 (Histogram -SD- Layer 1); (e) F187 (Histogram -Entropy- Layer 1). Lines in boxes represent medians and the boundaries of the boxes represent lower and upper quartiles. "+" stands for outliers.